Fish and Shellfish Immunology 131 (2022) 672–681

Contents lists available at ScienceDirect

Fish and Shellfish Immunology

journal homepage: www.elsevier.com/locate/fsi

Full length article

Generation of viperin-knockout zebrafish by CRISPR/Cas9-mediated genome engineering and the effect of this mutation under VHSV infection

K.A.S.N. Shanaka [a,b,1], Sumi Jung [a,b,1], K.P. Madushani [a,b], H.M.S.M. Wijerathna [a,b], M.D. Neranjan Tharuka [a,b], Myoung-Jin Kim [c,**], Jehee Lee [a,b,*]

[a] Department of Marine Life Sciences & Fish Vaccine Research Center, Jeju National University, Jeju Self, Governing Province, 63243, Republic of Korea
[b] Marine Science Institute, Jeju National University, Jeju Self-Governing Province, 63333, Republic of Korea
[c] Nakdonggang National Institute of Biological Resources, Sangju-si, Gyeongsangbuk-do, 37242, Republic of Korea

ARTICLE INFO

Keywords:
Zebrafish
VHSV
Viperin
Knockout model
CRISPR/Cas9

ABSTRACT

Viperin is an important virus-induced protein in animals that negatively participates in RNA viral replication and transcription. The reactive machinery of viperin suggests that it produces a regulatory molecule ddhCTP, which may affect immune regulation. In this study, we investigated the expression pattern of *viperin* in larval and adult stages of zebrafish by whole-mount *in situ* hybridization and reverse transcription-quantitative PCR (RT-qPCR). To elucidate the function of viperin, we generated a zebrafish knockout model using the CRISPR/Cas9 method and evaluated the mutation's effects under viral hemorrhagic septicemia virus (VHSV) infections. In zebrafish larvae, *viperin* was expressed in the brain region, eye, and pharynx, which was confirmed by cryosectioning. In adult zebrafish, blood cells showed the highest levels of *viperin* expression. In 5 dpf fish challenged with VHSV, the expression of the viral *NP* protein was significantly enhanced in viperin$^{-/-}$ compared to wild-type fish. *In vitro* VHSV propagation analysis indicated comparatively higher levels of virus propagation in viperin$^{-/-}$ fish. Mortality analysis confirmed higher mortality rates, and interferon gene expression analysis showed a strong upregulation of *interferon (ifn)φ1* and *3* gene in viperin$^{-/-}$ fish infected with VHSV. This study describes the successful generation of a viperin-knockout model and the role of viperin during VHSV infections.

1. Introduction

Viperin is a virus-induced protein thought to have originated from ancient metabolic enzymes [1]. This protein bears a highly conserved Cx_3Cx_2C motif, known as the catalytic motif, of which three cysteine amino acids can incorporate the 4Fe–4S cluster, which is key to viperin's catalytic reaction. The mechanisms proposed for viperin illustrates the ability to produce a di-deoxy nucleotide, ddhCTP, from dhCTP. The lack of a 3′-hydroxyl group makes ddhCTP a universal chain terminator nucleotide for RNA polymerization reactions [2].

Single-stranded RNA viruses, either positive or negative, propagate by RNA-dependent RNA synthesis, in which a unique class of RNA polymerases called RNA-dependent RNA polymerases (RdRps) are employed. As the mechanism of RdRp deviates from the eukaryotic RNA processing, the evolution of antiviral defense mechanisms may have targeted this RNA-dependent RNA synthesis machinery [3]. ddhCTP produced by viperin can bind to RdRp to inhibit viral RNA synthesis [4].

Several studies have delineated the catalytic function of viperin in mammals [5], reptiles [6], birds [7], and fish [8]. These studies suggest a repertoire of catalyzed mechanisms, including direct inhibition of viral transcription and replication [9], lipid vesicle formation modulation [10], alterations to metabolism [11], and several antiviral regulatory functions [1]. It remains unclear how a single protein with a single catalytic domain could possess all these functions. Although ddhCTP may explain viperin's ability to target a single-stranded RNA virus and inhibit its transcription and replication machinery, few studies have evaluated the additional functions of viperin, which would undoubtedly shed light on its regulatory mechanisms *in vivo* [12].

Compared to mammalian viperin, the expression regulation of viperin and its role in lower vertebrates, including fish, is lesser-known. Viral infection or stimulation with RNA virus mimicry materials such as poly I:C caused substantial expression of *viperin* in fish cells or *in vivo*

* Corresponding author. Marine Molecular Genetics Lab, Department of Marine Life Sciences, Jeju National University, Jeju, 63243, Republic of Korea.
** Corresponding author.
E-mail addresses: mjkim@nnibr.re.kr (M.-J. Kim), jehee@jejunu.ac.kr (J. Lee).
[1] These authors have contributed equally to this work.

https://doi.org/10.1016/j.fsi.2022.10.040
Received 15 July 2022; Received in revised form 17 October 2022; Accepted 19 October 2022
Available online 26 October 2022

models. Promoter regions of the fish viperin gene, including that of zebrafish, have identified interferon response elements (ISRE), indicating fish ifn has a regulatory role on the viperin expression [13,14].

Viral hemorrhagic septicemia virus (VHSV) is a deadly pathogen in both free-living and cultured fish [15]. A considerable loss of aquaculture species due to VHSV infection has been reported; therefore, studies focusing on antiviral genes are of paramount importance in understanding natural defense route and establishing effective treatment strategies [16]. Furthermore, a comprehensive understanding of antiviral mechanisms is vital in the development of virus-specific drugs, vaccines, and genomic selection of aquaculture species. Hence, our study was aimed at describing the role of viperin in zebrafish. First, the expression pattern of *viperin* was determined using whole-mount *in situ* hybridization (WISH) and reverse transcription-quantitative PCR (RT-qPCR). To analyze its function, we generated a *viperin*-knockout zebrafish model (KO), and it was infected with VHSV to evaluate viral gene transcription. We also assessed the gene expression alteration in viperin-KO. This study provides a suitable model to elucidate the role of viperin in antiviral defense mechanisms, and our findings could aid the development of antiviral treatment strategies.

2. Materials and methods

2.1. Bioinformatic analysis

The genomic sequence for zebrafish *viperin* was obtained from the ZFIN server (https://zfin.org). Homology models for viperin were constructed using the SWISS-MODEL online server (https://swissmodel.expasy.org). PyMOL (version 2.5) was used to visualize the models (https://pymol.org). Homology structures for zebrafish viperin were analyzed with the CAVER tool [17]. Orthologous *viperin* sequences obtained from the NCBI database (https://www.ncbi.nlm.nih.gov/nucleotide) were used to construct a phylogenetic tree using MEGA (version 10) (https://www.megasoftware.net). For the phylogenetic tree, orthologous sequences were aligned using the clustalW algorithm (https://www.ebi.ac.uk/Tools/msa/clustalo). For the tree construction, the neighbor-joining method with 5000 bootstrap replicates was used. The equal input model was used as the substitution model, and the rates were homogenized. For the tree evaluation, each organism in the tree was checked to reside in its natural classification groups, and the bootstrap values were used to evaluate the branching pattern.

2.2. Zebrafish husbandry

Larval and adult wild-type (WT, AB) zebrafish were maintained as previously described [18]. The light/dark cycle, water temperature, pH, and conductivity were maintained at constant levels (14:10, 28 ± 0.5 °C, pH 6.8–7.5, and 500–800 μS, respectively). Fish were fed a live Artemia diet three times per day. The study protocol was approved by the Jeju National University Animal Ethics Committee.

2.3. Whole-mount in situ hybridization (WISH) and cryosectioning

A digoxigenin-labeled antisense probe for *viperin* was synthesized by *in vitro* transcription. Larval developmental stages, including 24 hpf, 3 dpf, and 5 dpf, were separated, and the 3 dpf and 5 dpf stages were treated with 0.003% phenylthiourea (Sigma-Aldrich, USA) at 24 hpf. Embryos were anesthetized with MS-222 (Tricaine, Sigma-Aldrich), transferred into 4% paraformaldehyde for 24 h at 4 °C, and then transferred to a 100% methanol solution.

WISH was performed as previously described [19], with slight modifications. After imaging for WISH, embryos were fixed in agarose. Agarose blocks were equilibrated in a 30% sucrose solution (Sigma) and instantly frozen in liquid nitrogen. The frozen blocks were stored at −80 °C until sectioning was performed using a cryostat (CM3050 S, Leica, Germany).

2.4. Generation of viperin$^{-/-}$ fish

CCTop (https://crispr.cos.uni-heidelberg.de) was used to design single-guide RNA (sgRNA, Supplementary Table 1), which was then synthesized as previously described [20]. sgRNA at a final concentration of 100 ng/μL was mixed with 1 μL of recombinant Cas9 protein (including (KCl 100 mM and 0.05% phenol red, ToolGen, South Korea) and injected into one-cell-stage embryos using a micro-injector (Pico Pump, World Precision Instruments, USA). After 24 h, the efficiency of mutagenesis in the F0 fish was analyzed using the T7 endonuclease [21].

F0 fish were crossed with WT fish, and their embryos were genotyped using PCR. F0 fish positive for the mutation were identified, and embryos were selected for the F1 generation. The F1 generation was sequenced to detect the mutation, and only the initial frameshift mutation of viperin was selected as the candidate mutation. The F2 generation was obtained by crossing F1 × F1 individuals and screened for the homologous mutation of the *viperin* gene *(viperin$^{-/-}$)*. F2 fish with this mutation were separated, and embryos for experiments (F3 generation) were obtained by crossing viperin$^{-/-}$ × viperin$^{-/-}$ fish (Supplementary Fig. 1).

2.5. VHSV culturing and stock preparation

VHSV (Genotype IVa, FWando05, NCBI- FJ811900.2) was grown in FHM cells (20 °C, atmospheric conditions) in L-15 medium supplemented with 5% FBS, 1% streptomycin, and 1% penicillin. Cells were incubated until all cells were detached from the flask bottom and floating in the medium. The cell-containing solution was collected, subjected to three freeze-thaw cycles (frozen to −80 °C), vortexed, filtered through a 20 μm filter, and stored at −80 °C until the infection experiment.

2.6. VHSV challenge experiment

To examine virus propagation in viperin$^{-/-}$ fish, we collected 50 embryos per treatment group and incubated these at 28 °C for three days. The fish larvae were subsequently transferred to a 20 °C incubator and injected with equal amounts of VHSV at the 4 dpf stage using a calibrated micro-injector (Supplementary Fig. 2). Approximately 3000 $TCID_{50}$ VHSV/larvae were injected and incubated at 18 °C until RNA extraction. Post-injection fish survival was recorded daily.

rVHSV-ΔNV-EGFP (IVa) was kindly donated by the Department of Aquatic Life Medicine and the Department of Marine Biomaterials & Aquaculture, Pukyong National University, Busan, South Korea [22]. rVHSV-ΔNV-EGFP was propagated under conditions similar to those used for WT VHSV. rVHSV was injected into the yolk of the 4 dpf larvae. For the immersion experiment, we generated a neutrophile-labeled transgenic viperin$^{-/-}$ fish by crossing with *Tg(mpx:mCherry)* line. A tissue injury in fish was introduced by caudal fin amputation and immersed in 10^8 $TCID_{50}$/mL rVHSV at 18 °C. Fluorescent microscopy (40 ×, Leica Microsystems, Germany) was used for imaging, and images were modified for presentation using the Leica Application Suite X software (version 3.3).

2.7. Extraction of VHSV from zebrafish larvae

Thirty larvae (n=30) were collected in a homogenizing tube, and 1 mL of L-15 plain media (1% P/S) was added. The sample was then homogenized and frozen at −80 °C. Three freeze-thaw cycles were performed, samples were filtered through 20 μm filters, and the filtrate was stored at −80 °C.

2.8. Calculating $TCID_{50}$/mL

FHM cells were cultured in 96-well plates. At a cell confluency of 90%, cells were infected with 10-fold dilutions (from 10^{-1} to 10^{-8}) of

VHSV, and the emergence of cytopathic effects was assessed daily. After 7 d, cell viability was assessed using the crystal violet method [23]. $TCID_{50}$/mL was calculated as previously described [24].

2.9. Sample collection, RNA extraction, and cDNA synthesis

Fish were anesthetized with MS-222 (160 μg/mL) before sample collection. Tissue samples were immediately frozen in liquid nitrogen and stored at −80 °C. Following extraction with TRIzol reagent (Thermo Fisher Scientific, Waltham, MA, USA). Total RNA (3 μg) was used to synthesize cDNA using the PrimeScript 1st strand cDNA synthesis kit (Takara, Japan). cDNA was diluted 30-fold with nuclease-free water according to the Ct value for the respective reference gene (Supplementary Table 1). The diluted samples were then subjected to RT-qPCR.

2.10. Quantitative real-time PCR

Gene expression patterns were analyzed by RT-qPCR using a Dice™ TP800 Real-Time Thermal Cycler System (Takara, Japan). For each gene, primers were designed according to the minimum information for publication of quantitative real-time PCR experiments (MIQE) guidelines (Supplementary Table 1) [25].

2.11. Statistical analysis

All experiments were conducted at least three times. Data were analyzed using one-way analysis of variance (ANOVA) with Tukey's comparison ($p < 0.05$). Results labeled with lowercase letters differ significantly from other samples. The survival analysis was conducted

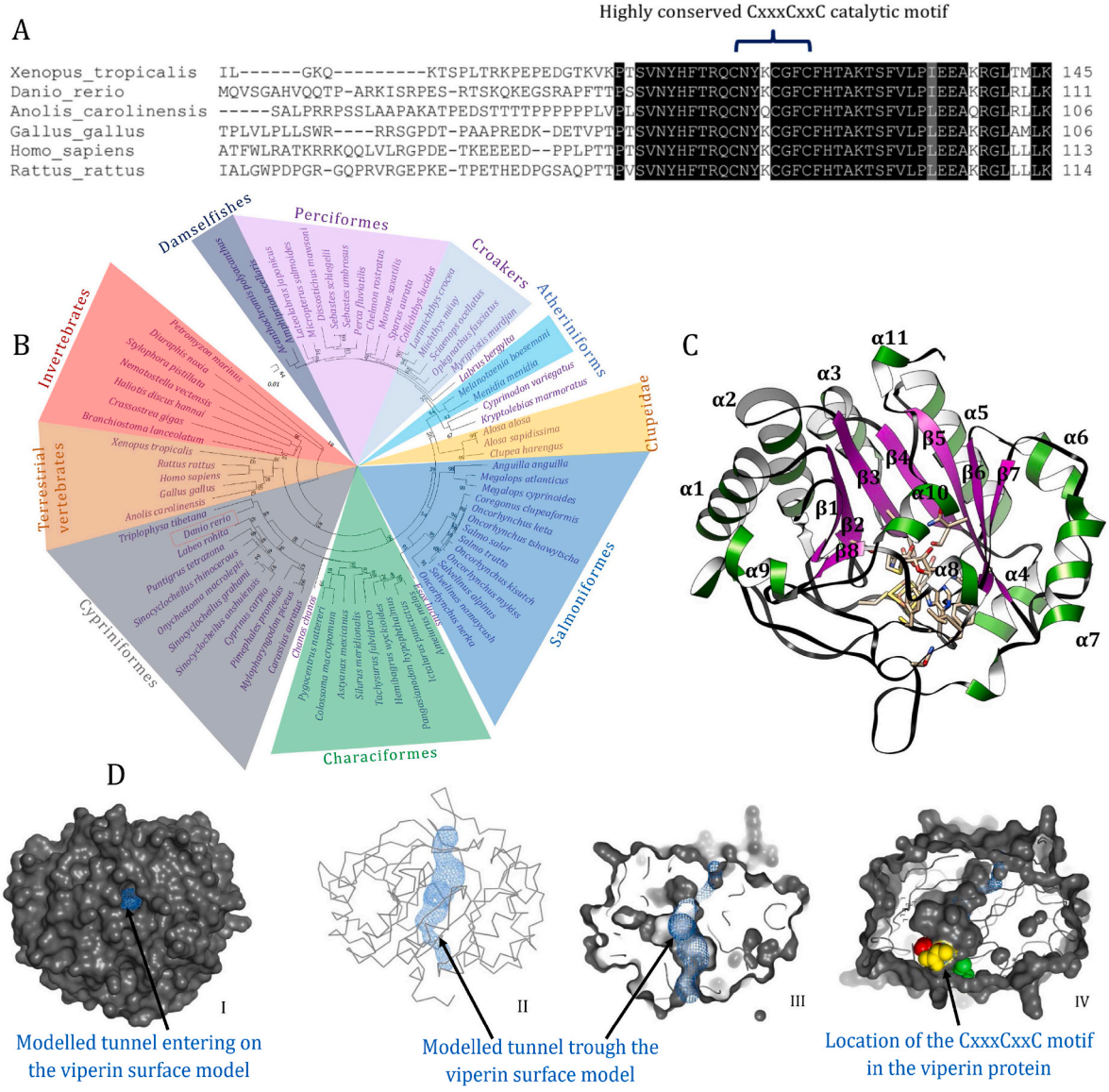

Fig. 1. Bioinformatic analysis of viperin. A, Multiple sequence analysis of *viperin* with *viperin* orthologs representing major vertebrate branches (Supplementary Table 2). The Cx_3Cx_2C motif region of *viperin* is highly conserved throughout the animal kingdom, which verifies the importance of this motif for the catalytic activity. **B,** Phylogenetic tree indicates the evolutionary position of *viperin* among certain fish species. As expected, zebrafish *viperin* was grouped with viperin homologs from the Cyprinidae family. The most closely related family is the Catostomidae. Furthermore, tetrapod *viperin* homologs are distantly related to fish homologs. This tree was replicated 5000 times, and the number at the nodes indicate their bootstrap values. **C,** Homology model showing the arrangement of secondary structural elements. Viperin bears 11 α-helices and 8 β-sheets arranged in an outer and inner circle, respectively. Reference structures used for the model are mentioned in Supplementary Table 3. **D,** Structural analysis of viperin. **DI,** A surface model for viperin showing the tunnel at the center of the protein structure. **DII,** and **DIII,** the tunnel (blue mesh) at the center of the viperin structure. **DIV,** The relative position of the cysteine amino acids (green, yellow, and red) in the catalytic motif.

using the Kaplan–Meier method, and the data were analyzed using the Mantel–Cox test ($p < 0.0001$).

3. Results and discussion

3.1. Bioinformatic analysis

The genomic region where *viperin* is located contains six exons that produce a coding sequence (CDS) of 1080 nucleotides. The viperin CDS codes for a protein with 359 amino acids, in which three domains were identified. The N-terminal domain contains an endoplasmic reticulum (ER) localization signal sequence (amino acids 1–38) that facilitates viperin localization into the ER. Most viruses use the ER for replication, protein synthesis, and propagation [26]. Therefore, localization to the ER is logistically plausible. The middle catalytic domain is highly consistent with other viperin proteins; the main motif in this catalytic domain is the characteristic Cx_3Cx_2C motif (amino acids 81–88) (Fig. 1A). Although the sequence of the C-terminal domain (89–359) is conserved with other known viperin proteins, its function remains unclear. Multiple functions have been described for the C-terminal domain, including virus protein binding [27], oligomerization [28], and antiviral activity toward specific viruses [29]. According to the phylogenetic analysis (Fig. 1B), *viperin* occurred in the same clade as proteins from the carp family (Cyprinidae). Other economically important fish, such as salmonids, occurred in separate clades to that of *viperin*, indicating their viperin sequences are different from that of zebrafish. Furthermore, mammalian viperin protein sequences were distantly related to zebrafish *viperin*.

In mammals, viperin proteins act as ddhNTP synthases. Strong similarities between the catalytic regions of *viperin* and its mammalian

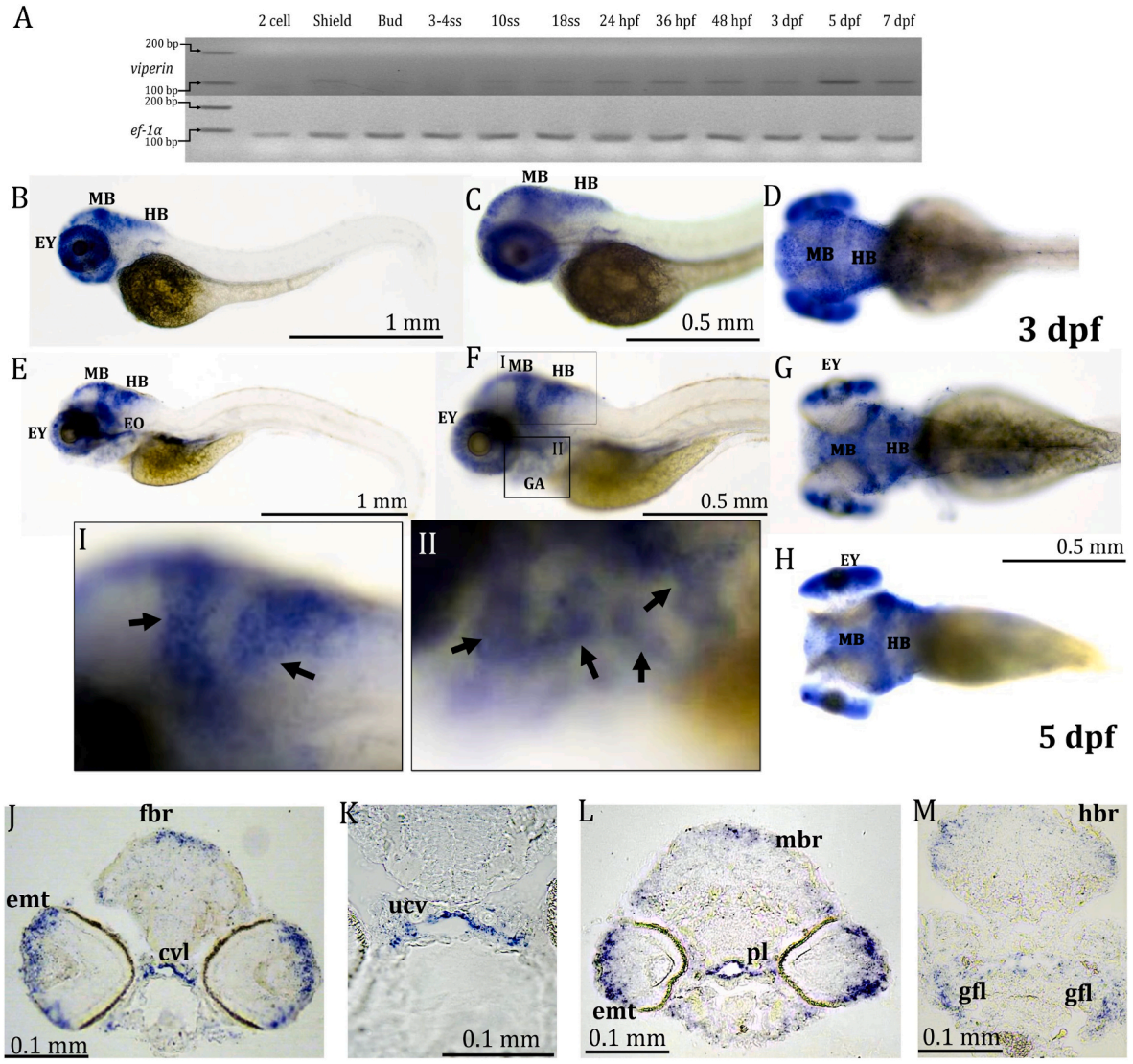

Fig. 2. *Viperin* expression pattern at different developmental stages. A, In WT fish, *viperin* was strongly expressed as early as the shield stage. At 5 dpf, *viperin* showed a relatively higher expression compared to other developmental stages. **B,** Whole-mount *in situ* hybridization of 3 dpf zebrafish larvae. Expression of *viperin* is mainly observable in the midbrain (MB) and hindbrain (HB) regions of 3 dpf zebrafish larvae. Other than the brain, the eye (EY) showed a considerable expression. **C,** High magnification of the head region of 3 dpf fish. **D,** Dorsal view of 3 dpf larvae. **E,** Whole-body image of a 5 dpf larvae showing considerable expression pattern in the MB, HB, EY, and esophagus (EO). **F,** high magnification image of the head region showing an expression in the MB, HB, EO, and visceral/gill arch (GA) region. **F-1,** Zoom-in image of the brain region. **F-II,** Zoom-in image of the internal tissue region indicating the GA. Black arrows are indicating the significant expression. Dorsal (**G**) and ventral (**H**) views of the 5 dpf embryo showing the expression of viperin in the MB and HB regions. **J,** Transverse section of the forehead region showing viperin expression in forebrain region (fbr), eye mucosal tissue (emt), and cranial cavity lining (cvl). **K,** high magnification image for the expression in upper cell layer of the cranial cavity (ucv). **L,** Transverse section of the MB region indicating the viperin expression in the eye mucosal tissue and the pharynx (pl). **M,** transverse section of the larvae in the HB region indicating the viperin expression in the hind brain (hbr) and the visceral/gill filaments (gfl).

counterparts suggest that viperin could act as a ddhNTP synthase in zebrafish [30]. Radical SAM enzymes use two major components to initiate various reactions, i.e., 4Fe–4S cluster and S-adenosylmethionine, and our homology model supports the availability of both components. In *viperin*, three cysteine amino acids (C81, C85, and C88) at the catalytic motif form iron–sulfur bonds with three adjacent iron molecules in the 4Fe–4S cluster. These three iron atoms are interconnected via a single sulfur atom. Iron–sulfur clusters generate a range of reduction potentials (−400 to +400 mV) [31], which are used to catalyze various reactions. In viperin, the reduction potential of the iron–sulfur cluster is used to synthesize ddhCTP from dhCTP.

We analyzed *viperin in silico* to elucidate its structural features. The homology model of viperin comprised eight β-sheets and 11 α-helices. The α-helices and β-sheets are arranged as an outer and inner circle in the viperin structure (Fig. 1C). The distribution of α-helices and β-sheets showed a near symmetrical arrangement around the middle catalytic elements, suggesting that the α-helices may be involved in structural functions, such as the stabilization of viperin and its catalytic elements. We hypothesize that a radical reaction occurring inside the cell requires a specific microenvironment, the intermediate products formed during radical reactions are highly reactive and should occur separately to sensitive biomolecules. Further analysis revealed that viperin includes a central tunnel that passes through the protein structure (Fig. 1DI and DII). The catalytic center was present on the tunnel surface and exposed to the tunnel cavity (Fig. 1DIII and DIV). According to this structural arrangement, the reactants or products may enter through this tunnel, and viperin may proceed via a radical mechanism without interfering with the rest of the cell. Accordingly, this arrangement is vital for viperin to act as a radical protein.

3.2. Viperin expression pattern in WT fish at the larval stages

The expression pattern of *viperin* was analyzed (Fig. 2A) at 12 distinct embryonic stages. *viperin* was expressed in the early and later stages of embryonic development, including 5 dpf and 7 dpf. Compared to other developmental stages, the 5 dpf fish showed relatively higher *viperin* expression. Usually, zebrafish hatch at 48–72 hpf [32], exposing the developing larvae to the external environment, and gut bacterial colonization usually occurs at 4 dpf. To compensate for this exposure, antiviral gene expression may be important specifically at around 5 dpf [33]. However, it is unclear whether *viperin* expression results from exposure to immune stimulants from the external environment or whether it is a developmental phenomenon. Therefore, further studies are required to fully understand this expression pattern.

We performed WISH for three zebrafish developmental stages. In embryos at 1 dpf, very low signals were observed 24 h after staining (data not shown). According to the results at 3 dpf, *viperin* was observed in the brain, eyes, and esophagus (Fig. 2B–D). In 5 dpf fish, the expression of *viperin* was observed in the eye, brain, esophagus, and gill arch (Fig. 2E–H).

According to the cryosectioning results (Fig. 2J-M), the mucosal tissue association of *viperin* was further verified in 5 dpf embryos where it occurred on the eye surface, upper cell layer of the cranial cavity, around the lining of the esophagus, and gill filaments. These mucosal tissues are vital to organ function and are especially important in aquatic organisms, where they create a barrier between the organs and the external environment and provide the first line of defense against pathogens [34]. Previous studies have identified the involvement of innate immune cells in mucosal tissues [34]. We hypothesize that these mucosa-associated cell populations may have expressed *viperin* during the early stages of fish development when embryos are most sensitive to viral infections. The association between viperin and mucosal tissues has also been shown in humans, where it was detected in buccal mucosa cells [35]. This evidence further supports the results of the present study.

3.3. Expression pattern of viperin in adult zebrafish

We analyzed the tissue-specific expression of *viperin* in adult fish (Fig. 3) and found that the blood, spleen, testis, and brain showed the highest expression levels, and the kidneys and ovaries showed the lowest expression levels.

Several studies conducted on fish have indicated that viperin expression is the highest in the blood [36,37]. Blood serves as a medium for virus propagation, and virus-infected blood cells can move freely until they are recognized by the adaptive immune system, making viral entry into blood cells particularly lethal. Therefore, enhanced antiviral mechanisms are expected to occur in the blood, where several naturally occurring immune cells produce antiviral proteins, such as viperin. Concurrently, these findings may explain the observed expression levels of *viperin* in the blood.

The observed expression in the spleen may be related to its expression in the blood, as blood is filtered through the spleen. During WISH, we observed higher expression levels in the brain. Adult fish also showed considerable expression of *viperin* in the brain, indicating that this expression pattern was retained during development. In contrast to its expression in the gut of adult fish, we could not find any expression of *viperin* in the gut of 5 dpf fish based on cryosectioning. This difference in expression pattern may be associated with the transition to active feeding as this promotes an animal's exposure to antigens. The fish gut serves as one possible route for viral infections in adult fish [38], and the active omnivorous feeding behavior of zebrafish increases the potential for infection. Thus, *viperin* expression in the gut may be important for antiviral defense, especially in adult fish.

3.4. Genotyping and sequencing of viperin$^{-/-}$ fish

After microinjection with sgRNA, the efficiency of mutagenesis was determined by PCR, followed by hetero-duplex formation using T7 endonuclease. F1 fish were genotyped by PCR, and positive fish were sequenced to identify the type of mutation generated. Two mutations were identified, a frameshift (4 bp deletion) (Fig. 4A) and a non-frameshift mutation (15 bp deletion), of which only the early frameshift mutation was screened. F2 fish were genotyped by PCR, and fish homologous to viperin$^{-/-}$ were selected. Using RT-PCR, viperin$^{-/-}$ fish

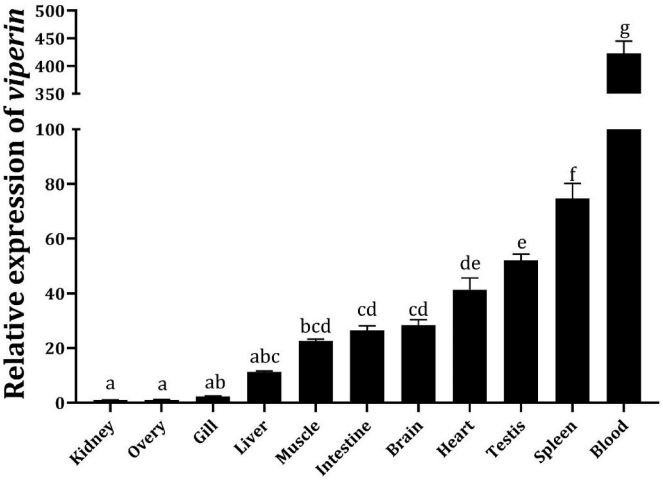

Fig. 3. The distribution of *viperin* in adult zebrafish tissues. The expression pattern of *viperin* was analyzed by qPCR, and the data was processed using the Livak method. Blood had the highest expression of *viperin*, with the spleen, testis, heart, intestine, and brain also showing significant levels of expression. The kidneys and ovaries had the lowest levels of expression. Data were normalized to the expression of the kidney. Data were analyzed with a one-way ANOVA and Tukey's comparison ($p < 0.05$). Results labeled with different lowercase letters differ significantly from other samples.

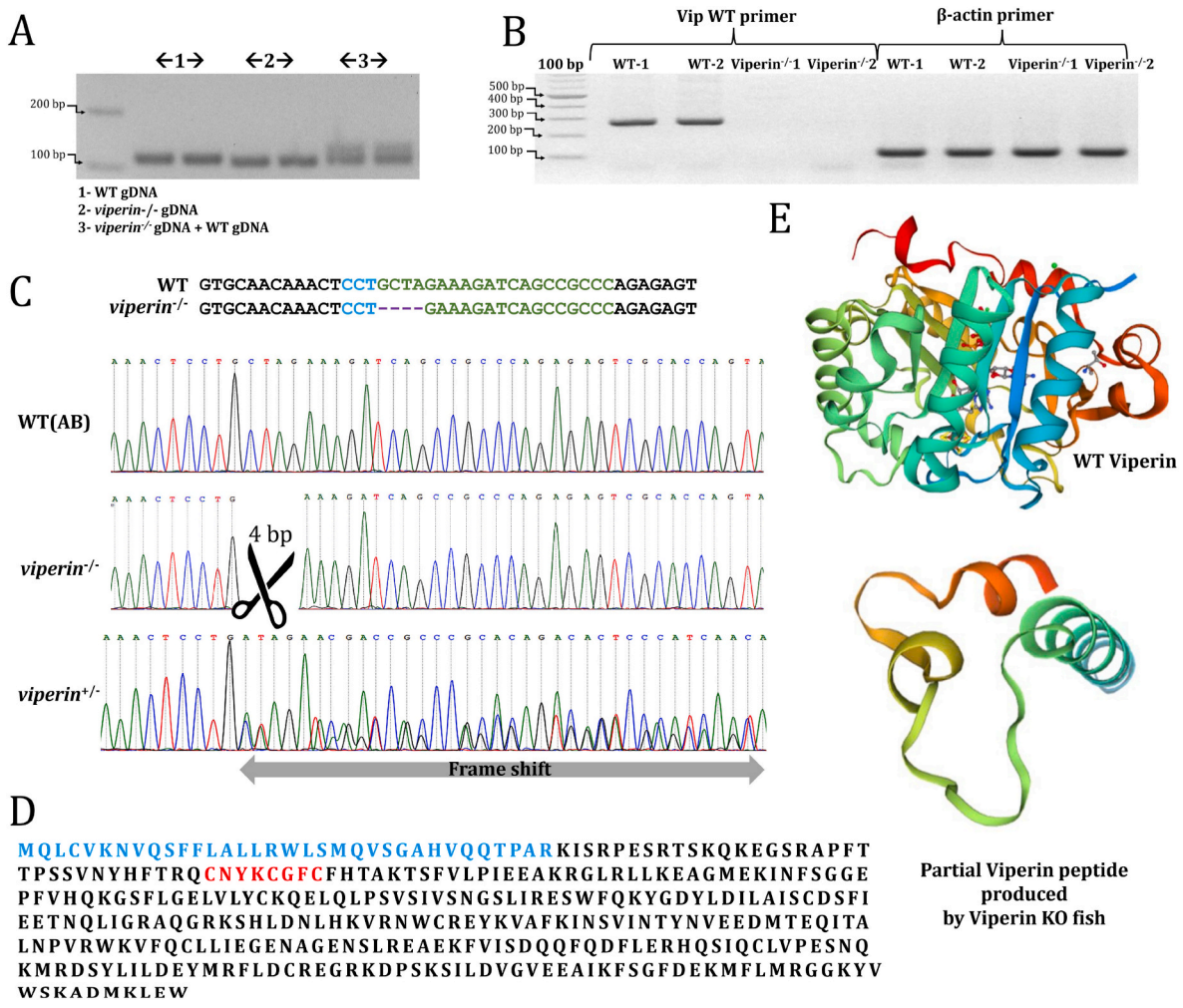

Fig. 4. Generation of viperin$^{-/-}$ fish. A, Verification of two PCR products from viperin$^{-/-}$ gDNA mixed with WT gDNA. **B,** Confirming the establishment of viperin$^{-/-}$ fish by RT-PCR, with *β-actin* used as reference gene. Total RNA was extracted from both WT and viperin$^{-/-}$ fish, and the expression of *viperin* was analyzed by RT-PCR. Viperin$^{-/-}$ fish completely lacked the wild-type (WT) *viperin* transcript. **C,** Type of mutation detected in the viperin$^{-/-}$ genome. The genomic region containing *viperin* was cloned and sequenced in both WT and viperin$^{-/-}$ fish, which indicated a 4 bp base pair deletion. Chromatogram for the viperin$^{-/-}$ indicate a 4 bp deletion at the point of mutation. Viperin$^{+/-}$ fish had mixed peaks after the region of 4 bp deletion. **D,** WT and mutated viperin protein (the extent of the sequence coded by the KO model is represented by blue letters). **E,** the mutated peptide produced by the KO model completely lacked the catalytic motif.

was analyzed to verify the absence of WT *viperin* transcripts (Fig. 4B). Using *in silico* analysis, we generated a protein model produced by the mutated transcript. The mutated transcript had an early translation stop signal, and the partial peptide produced by the mutated *viperin* transcript did not contain the catalytic domain (Fig. 4C–E) for ddhCTP production.

3.5. VHSV experiment

Considering the comparatively higher *viperin* expression level at around 5 dpf, we selected 4 dpf embryos for VHSV injection. We compared the morphology between WT and viperin$^{-/-}$ fish before the VHSV experiment and indicated no significant difference (Fig. 5A). This developmental time window should allow us to compare the effect of viperin on VHSV better than other developmental stages due to higher *viperin* expression and lack of morphological abnormalities.

Zebrafish larvae lack adaptive immune responses to mount antibody-mediated immunity [39]. Therefore, zebrafish larvae are particularly suitable models for studying innate immune proteins. Studies indicated the suitability of VHSV infection experiments in zebrafish [40]. Natural VHSV (IVa) infections occur bellow 15 °C [41]. For zebrafish larvae, an infection temperature of 18 °C is recommended for VHSV experiments [40]. Even if the temperature is reduced to 18 °C, the poikilothermic nature of fish causes less effect on the immune gene regulation [42]. This feature allows to use zebrafish to analyze the gene expression regulation under VHSV infections. In natural fish, VHSV infections mostly occur through fin bases, gills, or wounds in skin. After the initial exposure to VHSV, the virus then migrates into the blood vessels [15]. Immersion of viperin$^{-/-}$ larvae without tissue injury does not produce significant VHSV infection (data not shown). Therefore, we used microinjection into yolk and immersion in VHSV after caudal fin amputation. Injection into the yolk provided more consistent and stable infections, and we used this method for the gene expression analysis.

After VHSV microinjection, WT fish showed morphological abnormalities, such as hind yolk edema, similar to those previously described for virus-injected zebrafish larvae [43]. However, when viperin$^{-/-}$ fish were injected with VHSV, a higher degree of abnormalities was observed, including pericardial edema, cytosis, and hind yolk edema. Therefore, the pathological effects of VHSV were more severe in the absence of viperin (Fig. 5B).

Zebrafish larvae were injected with rVHSV-ΔNV-EGFP (genotype IVa), which expresses a green fluorescent protein (EGFP) during its propagation. We found that EGFP signals were more intense in viperin$^{-/-}$ than in WT larvae (Fig. 5C and D). In teleost fish, VHSV had tropism for

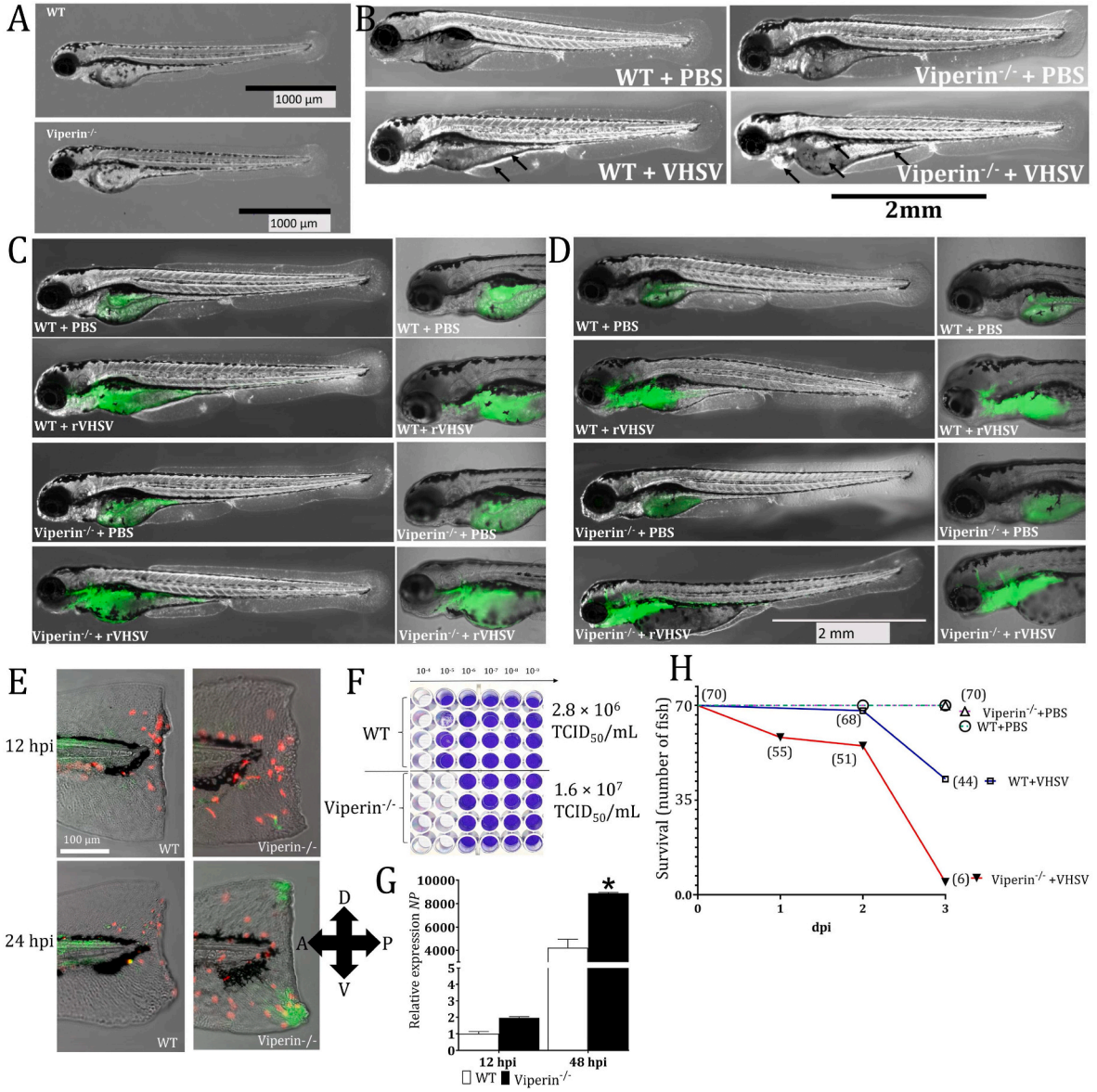

Fig. 5. VHSV infection of viperin$^{-/-}$ fish. A, Initial morphology of 4 dpf viperin$^{-/-}$ fish showed no abnormal phenotype. **B,** at 4 dpf, the KO and control fish were injected with VHSV. Morphology was recorded at 2 dpi. Viperin$^{-/-}$ fish showed more severe abnormalities, such as yolk edema, hind yolk edema, cytosis, and cardiomegaly (indicated with arrows). **C,** rVHSV-ΔNV-EGFP (rVHSV) was injected into 4 dpf fish yolk, and the migration of the rVHSV was monitored through fluorescent microscopy at 30 hpi. **D**, rVHSV migration at 48 hpi. Viperin$^{-/-}$ fish showed a stronger EGFP signal compared to WT fish. **E,** rVHSV infection in the immersion experiment. The caudal fin of 4 dpf larvae was amputated and infected with rVHSV by immersion. Red color indicates attracting neutrophils toward the infection site. According to results, viperin$^{-/-}$ fish showed a higher infection at 30 hpi. **F,** VHSV was extracted from 30 larvae, and $TCID_{50}$/mL was calculated. Viperin$^{-/-}$ fish showed higher VHSV titers compared to WT fish. **G,** VHSV *NP* gene expression in viperin$^{-/-}$ vs WT fish injected with VHSV. *NP* gene was significantly higher in viperin$^{-/-}$ fish compared to WT fish at 48 hpi. Data were analyzed with a one-way ANOVA and Tukey's comparison ($p < 0.05$). Asterisks (*) indicate the significant difference. **H,** Survival rates during VHSV infection. After the VHSV injection, the survival of the fish was analyzed for 3 days (n = 70). According to the analysis, viperin$^{-/-}$ fish had significantly lower survival rates compared to WT fish. The fish that survived the experiment were mentioned within the brackets. The Kaplan–Meier method was used for survival analysis ($p < 0.0001$, Mantel–Cox test).

internal tissues such as the kidney, spleen, heart, liver, gastrointestinal tract, and brain ventricles [44,45]. Our result indicated that the heart, spleen, eye lining, kidney, brain ventricles, and gut regions have VHSV tropism in both WT and viperin$^{-/-}$ zebrafish, and a more intense signal was observed in the brain region of viperin$^{-/-}$ fish (Fig. 5D). Morphological abnormalities, such as edema, of various tissues indicate a higher degree of acute inflammatory responses in the viperin$^{-/-}$ than in WT fish. The strength of the morphological abnormalities corresponding to the EGFP signal strength indicated the high virus titer caused higher innate immune activation, such as expression of *ifn*, which is analyzed in the next section. We believe that elevated inflammatory activation in viperin$^{-/-}$ is triggered by higher virus titer.

In the injury immersion experiment, the relative strength and spread of VHSV were higher in viperin$^{-/-}$ fish than in WT fish (Fig. 5E). As caudal fin in 5 dpf fish comprised few cell layers, it provides a 2D platform to study the neutrophile migration. As VHSV proliferates progressively in the viperin$^{-/-}$ fish, more cytokines are produced at the infection site, recruiting more neutrophils. Importantly, the lack of viperin does not seem to interfere with the neutrophile accumulation at the infection site.

Next, we extracted VHSV from 3 dpi fish and quantified the titer using the $TCID_{50}$ method. According to the results, WT fish had 2.8 ×

10^6 $TCID_{50}$/mL, and viperin$^{-/-}$ fish had 1.6 × 10^7 $TCID_{50}$/mL, representing an almost ten-fold increase in the VHSV titer in viperin$^{-/-}$ compared to that in WT fish (Fig. 5F). Virus titration further confirmed the higher EGFP signal observed in viperin$^{-/-}$ fish than in WT fish. As virus RdRp is involved in the VHSV genomic replication [46], higher virus titers are expected in the absence of viperin. We then analyzed VHSV gene expression at 12 hpi and 48 hpi and found a significantly higher *NP* transcript at 48 hpi in viperin$^{-/-}$ than in WT larvae (Fig. 5G). This result agrees with the role of RdRp on the viral gene transcription. The lack of viperin may have caused RdRp to proceed with viral gene expression without interfering with ddhCTP.

We analyzed the survival of viperin$^{-/-}$ fish infected with VHSV and found that the majority of viperin$^{-/-}$ zebrafish larvae died within 3 d post-injection (Fig. 5H). Our findings indicate that viperin is crucial for survival during the early stages of zebrafish development, similar to the findings for other innate immune proteins [47]. During the rVHSV injection experiment, we observed the progressive EGFP toward the brain region in viperin$^{-/-}$. VHSV-infected fish in previous studies have shown severe tissue alterations like necrotic degeneration of the kidney and spleen [48]. Further, mechanisms such as autophagy and necrosis have been illustrated in cells infected with VHSV [49,50]. This type of cell damage might have caused higher mortality in the viperin$^{-/-}$ fish.

3.6. Zebrafish gene expression pattern in viperin$^{-/-}$ fish under VHSV infection

Under VHSV infection, the expression levels of *ifnφ1* and *ifnφ3* were significantly upregulated in WT fish (Fig. 6) and were significantly higher in viperin$^{-/-}$ than in WT fish, corresponding to the significant upregulation of *NP* and the strong EGFP signal in viperin$^{-/-}$ fish. We also analyzed the expression patterns of *ifnφ2* and *ifnφ4*, but their Ct values were greater than 30 cycles (Supplementary Table 4), indicating a comparatively lower levels of expression compared to *ifnφ1* or *ifnφ3*.

Several studies have described the ability of viperin to form a complex in the cytoplasm with IRAK1 and TRAF6, which are also associated with lipid bodies. This complex can transmit signals from MyD88-mediated virus RNA sensing and transcribe type-I IFN in mammals. Therefore, a lack of viperin can inhibit Myd88-mediated *ifn* expression [51,52]. One consideration is that the complex formation mechanism is relatively slow compared to *ifn* induction through *mavs* [52]. The higher virus titer in viperin$^{-/-}$ fish at 48 h may have triggered the strong expression of *ifn* through Mavs. A study conducted in a viperin-KO murine model indicated similar upregulation of *IFNβ* with the presence of dengue virus (DENV) [53].

To further support the enhanced *ifn* production in viperin$^{-/-}$ fish, we analyzed the *myeloperoxidase* (*mpx*) expression. Mpx is a marker for neutrophil activation [54,55]. According to the results, *mpx* transcripts in viperin$^{-/-}$ fish were significantly higher, indicating a higher activation of neutrophils in the viperin-KO fish due to higher VHSV titer.

Cytidine monophosphate (UMP-CMP) kinase-2 (*cmpk2*) produces the substrate for viperin [56]. Zebrafish genomic analysis indicated that *viperin* is located at chromosome 17 adjacent to mitochondrial *cmpk2*. This may indicate that viperin is grouped with Cmpk2 during its reactive mechanism. We found that the expression of *cmpk2* was significantly higher in viperin$^{-/-}$ than in WT fish at 48 hpi. To verify this observation, we analyzed the expression patterns of *viperin*, *cmpk2*, and *NP* in VHSV-injected adult zebrafish and found a similar pattern of expression (Supplementary Fig. 3). This suggests a common regulatory mechanism for *viperin* and *cmpk2* during viral infection [57]. Studies in humans have identified a regulatory RNA called cmpk2 long non-coding RNA (lnc-RNA-cmpk2) near the genomic region of Cmpk2 [56]. Unfortunately, no lncRNAs have been identified in this region for zebrafish,

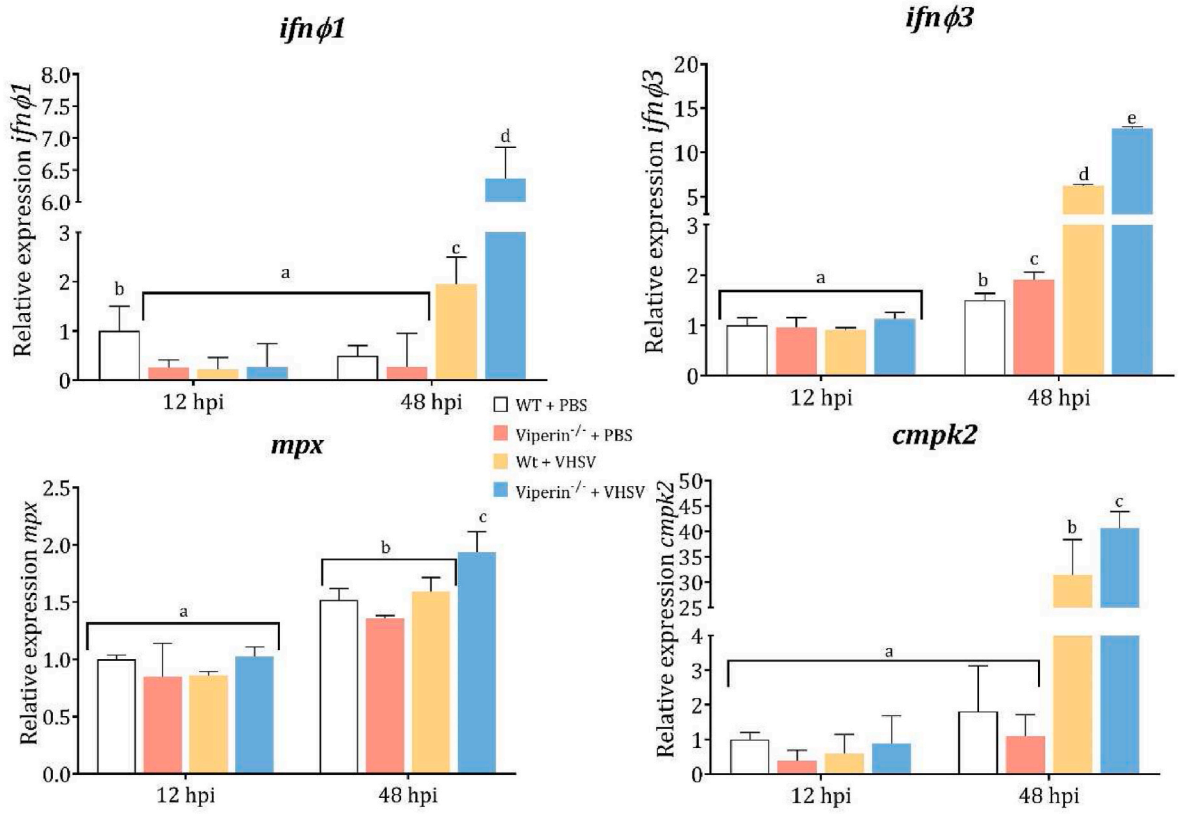

Fig. 6. Gene expression patterns in viperin$^{-/-}$ vs. WT fish. The average expression profile of *ifn*, *mpx*, and *cmpk2* at 12 hpi and 48 hpi *in vivo* (n = 50). In viperin$^{-/-}$ larvae injected with WT VHSV, both *ifnφ 1 and 3*, *mpx*, and *cmpk2* showed significant expression at 48 hpi. Gene expression levels were determined with RT-qPCR and analyzed using the Livak method. Data were normalized to the 12 hpi PBS-injected samples. Data were analyzed with a one-way ANOVA and Tukey's comparison ($p < 0.05$). Results labeled with different lowercase letters differ significantly from other samples.

though a long intergenic region away from the *cmpk2* and *viperin* pair may encode a non-coding-regulatory RNA, which could regulate the expression of both *viperin* and *cmpk2*.

4. Conclusions

In this study, we generated and characterized a zebrafish viperin-KO model to elucidate the role of viperin in teleost fish. *In silico* analysis revealed the presence of the Cx_3Cx_2C catalytic motif in the central catalytic tunnel of protein. According to WISH, *viperin* expression was detected mostly in mucosal tissue linings, such as the eye surface, upper layer of the cranial cavity, esophagus, and brain. CRISPR/Cas9 mutagenesis resulted a 4 bp frameshift deletion in the *viperin* coding sequence. When viperin$^{-/-}$ fish were challenged with VHSV, *NP* gene expression, virus distribution and titer were increased compared to WT fish. VHSV-injected viperin$^{-/-}$ fish larvae showed very low post-infection survival rates compared to WT fish. Gene expression analysis indicated significant upregulation of *ifn* genes in viperin$^{-/-}$ fish than WT fish. These findings verify the successful generation of a zebrafish viperin-KO model and reveal the important role of viperin during VHSV infections.

CRediT authorship contribution statement

K.A.S.N. Shanaka: Conceptualization, Methodology, Software, Formal analysis, Writing – original draft. **Sumi Jung:** Resources, Writing – review & editing, Supervision. **K.P. Madushani:** Conceptualization, Methodology, Software, Formal analysis, Writing – original draft. **H.M. S.M. Wijerathna:** Writing – review & editing. **M.D. Neranjan Tharuka:** Conceptualization, Methodology. **Myoung-Jin Kim:** Resources, Writing – review & editing, Supervision. **Jehee Lee:** Conceptualization, Investigation, Resources, Writing – review & editing, Supervision, Project administration, Funding acquisition.

Data availability

Data will be made available on request.

Acknowledgments

This study was supported by the Basic Science Research Program of the National Research Foundation of Korea (NRF) funded by the Ministry of Education (2019R1A6A1A03033553) and supported by Korea Institute of Marine Science & Technology Promotion (KIMST) funded by the Ministry of Oceans and Fisheries (20220570).

Appendix A. Supplementary data

Supplementary data to this article can be found online at https://doi.org/10.1016/j.fsi.2022.10.040.

References

[1] S. Ghosh, E.N.G. Marsh, Viperin, An ancient radical SAM enzyme finds its place in modern cellular metabolism and innate immunity, J. Biol. Chem. 295 (2020) 11513–11528, https://doi.org/10.1074/jbc.REV120.012784.
[2] J.-Y. Seo, R. Yaneva, P. Cresswell, Viperin: a multifunctional, interferon-inducible protein that regulates virus replication, Cell Host Microbe 10 (2011) 534–539, https://doi.org/10.1016/j.chom.2011.11.004.
[3] Y. Ren, X. Li, Z. Tian, Y. Xu, R. Zhang, Y. Li, Zebrafish as an animal model for the antiviral RNA interference pathway, J. Gen. Virol. 102 (2021), https://doi.org/10.1099/jgv.0.001552.
[4] B. Shu, P. Gong, Structural basis of viral RNA-dependent RNA polymerase catalysis and translocation, Proc. Natl. Acad. Sci. USA 113 (2016), https://doi.org/10.1073/pnas.1602591113.
[5] M.T. Nelp, A.P. Young, B.M. Stepanski, V. Bandarian, Human viperin causes radical SAM-dependent elongation of Escherichia coli , hinting at its physiological role, Biochemistry 56 (2017) 3874–3876, https://doi.org/10.1021/acs.biochem.7b00608.
[6] N.L. Milic, S. Davis, J.M. Carr, S. Isberg, M.R. Beard, K.J. Helbig, Sequence analysis and characterisation of virally induced viperin in the saltwater crocodile (Crocodylus porosus), Dev. Comp. Immunol. 51 (2015) 108–115, https://doi.org/10.1016/j.dci.2015.03.001.
[7] M. Shah, M.S.K. Bharadwaj, A. Gupta, R. Kumar, S. Kumar, Chicken viperin inhibits Newcastle disease virus infection in vitro: a possible interaction with the viral matrix protein, Cytokine 120 (2019) 28–40, https://doi.org/10.1016/j.cyto.2019.04.007.
[8] K. Eslamloo, A. Ghorbani, X. Xue, S.M. Inkpen, M. Larijani, M.L. Rise, Characterization and transcript expression analyses of atlantic cod viperin, Front. Immunol. 10 (2019), https://doi.org/10.3389/fimmu.2019.00311.
[9] M.R. Jumat, T.N. Huong, L.I. Ravi, R. Stanford, B.H. Tan, R.J. Sugrue, Viperin protein expression inhibits the late stage of respiratory syncytial virus morphogenesis, Antivir. Res. 114 (2015) 11–20, https://doi.org/10.1016/j.antiviral.2014.11.007.
[10] T.J. Grunkemeyer, S. Ghosh, A.M. Patel, K. Sajja, J. Windak, V. Basrur, Y. Kim, A. I. Nesvizhskii, R.T. Kennedy, E.N.G. Marsh, The antiviral enzyme viperin inhibits cholesterol biosynthesis, J. Biol. Chem. 297 (2021), 100824, https://doi.org/10.1016/j.jbc.2021.100824.
[11] J.-Y. Seo, P. Cresswell, Viperin regulates cellular lipid metabolism during human cytomegalovirus infection, PLoS Pathog. 9 (2013), e1003497, https://doi.org/10.1371/journal.ppat.1003497.
[12] J. Eom, J.J. Kim, S.G. Yoon, H. Jeong, S. Son, J.B. Lee, J. Yoo, H.J. Seo, Y. Cho, K. S. Kim, K.M. Choi, I.Y. Kim, H.Y. Lee, K.T. Nam, P. Cresswell, J.K. Seong, J.Y. Seo, Intrinsic expression of viperin regulates thermogenesis in adipose tissues, Proc. Natl. Acad. Sci. U. S. A. 116 (2019) 17419–17428, https://doi.org/10.1073/pnas.1904480116.
[13] B. Wang, Y.-B. Zhang, T.-K. Liu, J. Shi, F. Sun, J.-F. Gui, Fish viperin exerts a conserved antiviral function through RLR-triggered IFN signaling pathway, Dev. Comp. Immunol. 47 (2014) 140–149, https://doi.org/10.1016/j.dci.2014.07.006.
[14] Z. Li, X. Xu, L. Huang, J. Wu, Q. Lu, Z. Xiang, J. Liao, S. Weng, X. Yu, J. He, Administration of recombinant IFN1 protects zebrafish (Danio rerio) from ISKNV infection, Fish Shellfish Immunol. 29 (2010) 399–406, https://doi.org/10.1016/j.fsi.2010.04.020.
[15] L. Baillon, E. Mérour, J. Cabon, L. Louboutin, E. Vigouroux, A.L.F. Alencar, A. Cuenca, Y. Blanchard, N.J. Olesen, V. Panzarin, T. Morin, M. Brémont, S. Biacchesi, The viral hemorrhagic septicemia virus (VHSV) markers of virulence in rainbow trout (Oncorhynchus mykiss), Front. Microbiol. 11 (2020), https://doi.org/10.3389/fmicb.2020.574231.
[16] Y. Li, C. Ran, K. Wei, Y. Xie, M. Xie, W. Zhou, Y. Yang, Z. Zhang, H. Lv, X. Ma, Z. Zhou, The effect of Astragalus polysaccharide on growth, gut and liver health, and anti-viral immunity of zebrafish, Aquaculture 540 (2021), 736677, https://doi.org/10.1016/j.aquaculture.2021.736677.
[17] J. Brezovsky, B. Kozlikova, J. Damborsky, Computational Analysis of Protein Tunnels and Channels, 2018, pp. 25–42, https://doi.org/10.1007/978-1-4939-7366-8_3.
[18] A. Avdesh, M. Chen, M.T. Martin-Iverson, A. Mondal, D. Ong, S. Rainey-Smith, K. Taddei, M. Lardelli, D.M. Groth, G. Verdile, R.N. Martins, Regular care and maintenance of a zebrafish (Danio rerio) laboratory: an introduction, J. Vis. Exp. (2012), https://doi.org/10.3791/4196.
[19] C. Thisse, B. Thisse, High-resolution in situ hybridization to whole-mount zebrafish embryos, Nat. Protoc. 3 (2008) 59–69, https://doi.org/10.1038/nprot.2007.514.
[20] G.K. Varshney, W. Pei, M.C. LaFave, J. Idol, L. Xu, V. Gallardo, B. Carrington, K. Bishop, M. Jones, M. Li, U. Harper, S.C. Huang, A. Prakash, W. Chen, R. Sood, J. Ledin, S.M. Burgess, High-throughput gene targeting and phenotyping in zebrafish using CRISPR/Cas9, Genome Res. 25 (2015) 1030–1042, https://doi.org/10.1101/gr.186379.114.
[21] M.F. Sentmanat, S.T. Peters, C.P. Florian, J.P. Connelly, S.M. Pruett-Miller, A survey of validation strategies for CRISPR-cas9 editing, Sci. Rep. 8 (2018) 888, https://doi.org/10.1038/s41598-018-19441-8.
[22] M. Kim, D. Kim, K. Kim, Generation and characterization of NV gene-knockout recombinant viral hemorrhagic septicemia virus (VHSV) genotype IVa, Dis. Aquat. Org. 97 (2011) 25–35, https://doi.org/10.3354/dao02394.
[23] 2016 M. Feoktistova, P. Geserick, M. Leverkus, Crystal violet assay for determining viability of cultured cells, Cold Spring Harb. Protoc. (2016), https://doi.org/10.1101/pdb.prot087379. pdb.prot087379.
[24] U. Karakus, M. Crameri, C. Lanz, E. Yángüez, Propagation and titration of influenza viruses, 59–88, https://doi.org/10.1007/978-1-4939-8678-1_4, 2018.
[25] S.A. Bustin, V. Benes, J.A. Garson, J. Hellemans, J. Huggett, M. Kubista, R. Mueller, T. Nolan, M.W. Pfaffl, G.L. Shipley, J. Vandesompele, C.T. Wittwer, The MIQE guidelines: minimum information for publication of quantitative real-time PCR experiments, Clin. Chem. 55 (2009) 611–622, https://doi.org/10.1373/clinchem.2008.112797.
[26] M.S. Ravindran, P. Bagchi, C.N. Cunningham, B. Tsai, Opportunistic intruders: how viruses orchestrate ER functions to infect cells, Nat. Rev. Microbiol. 14 (2016) 407–420, https://doi.org/10.1038/nrmicro.2016.60.
[27] S. Wang, X. Wu, T. Pan, W. Song, Y. Wang, F. Zhang, Z. Yuan, Viperin inhibits hepatitis C virus replication by interfering with binding of NS5A to host protein hVAP-33, J. Gen. Virol. 93 (2012) 83–92, https://doi.org/10.1099/vir.0.033860-0.
[28] A.M. Patel, E.N.G. Marsh, The antiviral enzyme, viperin, activates protein ubiquitination by the E3 ubiquitin ligase, TRAF6, J. Am. Chem. Soc. 143 (2021) 4910–4914, https://doi.org/10.1021/jacs.1c01045.
[29] B. Vanwalscappel, G. Gadea, P. Desprès, A viperin mutant bearing the K358R substitution lost its anti-ZIKA virus activity, Int. J. Mol. Sci. 20 (2019) 1574, https://doi.org/10.3390/ijms20071574.

[30] J.C. Lachowicz, A.S. Gizzi, S.C. Almo, T.L. Grove, Structural insight into the substrate scope of viperin and viperin-like enzymes from three domains of Life, Biochemistry 60 (2021) 2116–2129, https://doi.org/10.1021/acs.biochem.0c00958.
[31] A.V. Crain, K.S. Duschene, J.W. Peters, J.B. Broderick, Iron-sulfur cluster proteins, Fe/S-S-adenosylmethionine enzymes and hydrogenases, in: Encycl. Met., Springer New York, New York, NY, 2013, pp. 1034–1044, https://doi.org/10.1007/978-1-4614-1533-6_355.
[32] C.B. Kimmel, W.W. Ballard, S.R. Kimmel, B. Ullmann, T.F. Schilling, Stages of embryonic development of the zebrafish, Dev. Dynam. 203 (1995) 253–310, https://doi.org/10.1002/aja.1002030302.
[33] K.M. Balla, M.C. Rice, J.A. Gagnon, N.C. Elde, Linking virus discovery to immune responses visualized during zebrafish infections, Curr. Biol. 30 (2020) 2092–2103, https://doi.org/10.1016/j.cub.2020.04.031, e5.
[34] D. Gomez, J.O. Sunyer, I. Salinas, The mucosal immune system of fish: the evolution of tolerating commensals while fighting pathogens, Fish Shellfish Immunol. 35 (2013) 1729–1739, https://doi.org/10.1016/j.fsi.2013.09.032.
[35] SIB Swiss Institute of Bioinformatics, RSAD2 - ENSG00000134321 - Homo sapiens (human), (n.d.). https://bgee.org/gene/ENSG00000134321 (accessed June 21, 2022).
[36] K.A.S.N. Shanaka, M.D.N. Tharuka, T.T. Priyathilaka, J. Lee, Molecular characterization and expression analysis of rockfish (Sebastes schlegelii) viperin, and its ability to enervate RNA virus transcription and replication in vitro, Fish Shellfish Immunol. 92 (2019) 655–666, https://doi.org/10.1016/j.fsi.2019.06.015.
[37] E.R. Hinson, N.S. Joshi, J.H. Chen, C. Rahner, Y.W. Jung, X. Wang, S.M. Kaech, P. Cresswell, Viperin is highly induced in neutrophils and macrophages during acute and chronic lymphocytic choriomeningitis virus infection, J. Immunol. 184 (2010) 5723–5731, https://doi.org/10.4049/jimmunol.0903752.
[38] S. Mutoloki, H.M. Munang'andu, Ø. Evensen, Oral vaccination of fish – antigen preparations, uptake, and immune induction, Front. Immunol. 6 (2015), https://doi.org/10.3389/fimmu.2015.00519.
[39] N.S. Trede, D.M. Langenau, D. Traver, A.T. Look, L.I. Zon, The use of zebrafish to understand immunity, Immunity 20 (2004) 367–379, https://doi.org/10.1016/S1074-7613(04)00084-6.
[40] M.H. Marana, J.G. Schmidt, S. Biacchesi, N. Lorenzen, L. von G. Jørgensen, Zebrafish (Danio rerio) larvae as a model for real-time studies of propagating VHS virus infection, tissue tropism and neutrophil activity, J. Fish. Dis. 44 (2021) 563–571, https://doi.org/10.1111/jfd.13294.
[41] T. Ito, J. Kurita, K. Mori, N.J. Olesen, Virulence of viral haemorrhagic septicaemia virus (VHSV) genotype III in rainbow trout, Vet. Res. 47 (2016) 4, https://doi.org/10.1186/s13567-015-0303-z.
[42] B. Magnadottir, Immunological control of fish diseases, Mar. Biotechnol. 12 (2010) 361–379, https://doi.org/10.1007/s10126-010-9279-x.
[43] J. Van Dycke, A. Cuvry, J. Knickmann, A. Ny, S. Rakers, S. Taube, P. de Witte, J. Neyts, J. Rocha-Pereira, Infection of zebrafish larvae with human norovirus and evaluation of the in vivo efficacy of small-molecule inhibitors, Nat. Protoc. 16 (2021) 1830–1849, https://doi.org/10.1038/s41596-021-00499-0.
[44] J. Lovy, N.L. Lewis, P.K. Hershberger, W. Bennett, T.R. Meyers, K.A. Garver, Viral tropism and pathology associated with viral hemorrhagic septicemia in larval and juvenile Pacific herring, Vet. Microbiol. 161 (2012) 66–76, https://doi.org/10.1016/j.vetmic.2012.07.020.
[45] S.S.N. Qadiri, S.-J. Kim, R. Krishnan, J.-O. Kim, S. Kole, W.-S. Kim, M.-J. Oh, Localization and tissue tropism of viral haemorrhagic septicemia virus (VHSV) in experimentally infected juvenile olive flounder, Paralichthys olivaceus: an in situ hybridization and immunohistochemical study, Aquaculture 505 (2019) 242–252, https://doi.org/10.1016/j.aquaculture.2019.02.061.
[46] W. Zhang, L. Yao, X. Chen, M. Li, M. Yi, K. Jia, Functional characterization of myosin III light chain b of sea perch (Lateolabrax japonicus) in response to fish virus infection, Aquaculture 550 (2022), 737840, https://doi.org/10.1016/j.aquaculture.2021.737840.
[47] B. Novoa, A. Figueras, Zebrafish: model for the study of inflammation and the innate immune response to infectious diseases, 253–275, https://doi.org/10.1007/978-1-4614-0106-3_15, 2012.
[48] M. Faisal, M. Shavalier, R.K. Kim, E.V. Millard, M.R. Gunn, A.D. Winters, C. A. Schulz, A. Eissa, M.V. Thomas, M. Wolgamood, G.E. Whelan, J. Winton, Spread of the emerging viral hemorrhagic septicemia virus strain, genotype IVb, Mich. U. S.A, Viruses 4 (2012) 734–760, https://doi.org/10.3390/v4050734.
[49] P. García-Valtanen, M. del M. Ortega-Villaizán, A. Martínez-López, R. Medina-Gali, L. Pérez, S. Mackenzie, A. Figueras, J.M. Coll, A. Estepa, Autophagy-inducing peptides from mammalian VSV and fish VHSV rhabdoviral G glycoproteins (G) as models for the development of new therapeutic molecules, Autophagy 10 (2014) 1666–1680, https://doi.org/10.4161/auto.29557.
[50] J.F. Eléouët, N. Druesne, S. Chilmonczyk, D. Monge, M. Dorson, B. Delmas, Comparative study of in-situ cell death induced by the viruses of viral haemorrhagic septicaemia (VHS) and infectious pancreatic necrosis (IPN) in rainbow trout, J. Comp. Pathol. 124 (2001) 300–307, https://doi.org/10.1053/jcpa.2001.0467.
[51] J.J. Kim, K.S. Kim, J. Eom, J.B. Lee, J.-Y. Seo, Viperin differentially induces interferon-stimulated genes in distinct cell types, Immune Netw 19 (2019), https://doi.org/10.4110/in.2019.19.e33.
[52] K.J. Helbig, M.R. Beard, The role of viperin in the innate antiviral response, J. Mol. Biol. 426 (2014) 1210–1219, https://doi.org/10.1016/j.jmb.2013.10.019.
[53] W.-H. Al Shujairi, L.P. Kris, K. van der Hoek, E. Cowell, G. Bracho-Granado, T. Woodgate, M.R. Beard, J.M. Carr, Viperin is anti-viral in vitro but is dispensable for restricting dengue virus replication or induction of innate and inflammatory responses in vivo, J. Gen. Virol. 102 (2021), https://doi.org/10.1099/jgv.0.001669.
[54] Z. Wang, L. Lin, W. Chen, X. Zheng, Y. Zhang, Q. Liu, D. Yang, Neutrophil plays critical role during Edwardsiella piscicida immersion infection in zebrafish larvae, Fish Shellfish Immunol. 87 (2019) 565–572, https://doi.org/10.1016/j.fsi.2019.02.008.
[55] K.D. Buchan, T.K. Prajsnar, N.V. Ogryzko, N.W.M. de Jong, M. van Gent, J. Kolata, S.J. Foster, J.A.G. van Strijp, S.A. Renshaw, A transgenic zebrafish line for in vivo visualisation of neutrophil myeloperoxidase, PLoS One 14 (2019), e0215592, https://doi.org/10.1371/journal.pone.0215592.
[56] E.E. Rivera-Serrano, A.S. Gizzi, J.J. Arnold, T.L. Grove, S.C. Almo, C.E. Cameron, Viperin reveals its true function, Annu. Rev. Virol. 7 (2020) 421–446, https://doi.org/10.1146/annurev-virology-011720-095930.
[57] W. Liu, B. Chen, Chen li, J. Yao, J. Liu, M. Kuang, F. Wang, Y. Wang, G. Elkady, Y. Lu, Y. Zhang, X. Liu, Identification of fish CMPK2 as an interferon stimulated gene against SVCV infection, Fish Shellfish Immunol. 92 (2019) 125–132, https://doi.org/10.1016/j.fsi.2019.05.032.